Influence of Thermal Storage Tank Sizing on the Performance of Photovoltaic-Thermal Systems

Rafael William C. Faleiros[1], Bruna de O. Busson[2] and Júlio César Passos[3]

[1] Federal University of Santa Catarina, Florianópolis (Brazil)

Abstract

A thermal storage tank (TST) plays a key role in photovoltaic-thermal (PVT) systems, being responsible for storing heated water from PVT modules and improving the delivery of hot water to the point of consumption. The present study investigates how TST size affects the performance of a PVT system. Two configurations, each composed of one PVT module, a pump, and a TST with volumes of 300 L and 100 L, were tested under similar solar irradiance conditions. The 100 L TST heated up more rapidly, enhancing thermal efficiency in the early hours of the day; however, the thermal energy accumulation reduced the cooling capacity of the photovoltaic (PV) cells and consequently the electrical efficiency. In contrast, the 300 L TST, due to its higher thermal inertia, maintained more stable temperatures and smaller variations throughout the day, keeping the cells at lower temperatures and resulting in higher electrical efficiencies. These results highlight the dynamic behavior of the system, in which thermal and electrical efficiencies vary throughout the day according to the TST volume. The findings emphasize the importance of proper sizing of the TST volume to balance electrical and thermal energy outputs and provide experimental evidence to support future optimization of PVT systems for different demand profiles.

Keywords: PVT system, thermal storage tank, tank sizing, thermal efficiency, water tank temperature

1. Introduction

Recent debates have focused on the feasibility of transitioning to renewable energy sources as a means of reducing greenhouse gas emissions and decreasing dependence on fossil fuels (Atawi et al., 2024). Among the available options, solar energy has gained prominence as a versatile solution for the simultaneous generation of electricity and heat. This is primarily achieved through PV modules and solar thermal collectors, technologies commonly applied in both residential and industrial sectors (Samykano, 2023).

Conventional PV modules convert only part of the incident solar radiation into electricity, while the remaining energy is dissipated as heat by the system components (Tiwari et al., 2023). This thermal energy accumulation increases the operating temperature of PV cells, thereby reducing electrical performance due to the inverse relationship between temperature and efficiency (Michael et al., 2015). To mitigate this effect, PVT modules have been developed, capable of simultaneously generating electricity and recovering heat, thus reducing cell temperature and, consequently, improving electrical efficiency compared to conventional PV modules (Busson et al., 2024).

PVT systems generally consist of a PV module with a heat exchanger (HX) attached to the rear side, where the forced circulation of the working fluid removes excess heat, reducing the temperature of the PV cells and generating thermal energy (Erixno and Rahim, 2020). In this study, water is considered as the working fluid, while other research has investigated alternatives, for instance, the experimental use of nanofluids under tropical conditions has demonstrated improvements in both thermal and electrical performance compared to water (Al-Shamani et al., 2016).

In addition to these factors, the electrical and thermal performance of the system depends on the sizing of the TST, which affects the storage capacity, the thermal performance of the system, and its thermal inertia**.** Larger TSTs increase thermal inertia, providing more stable temperatures and favoring electrical performance by maintaining lower water temperatures and improving cell cooling throughout the day. In contrast, smaller TSTs heat up faster, increasing the water temperature and slightly improving thermal efficiency at certain periods, but reducing the cooling capacity of the working fluid and, consequently, the electrical efficiency (Cirrincione et al., 2020). This balance becomes even more critical in real-world applications, where electricity and hot

10.18086/swc.2025.02.18 Available at http://proceedings.ises.org

water demand profiles vary throughout the day.

Previous parametric studies have also indicated that both TST volume and water outlet flow significantly affect electrical efficiency (Barbu et al., 2020). Although previous studies have investigated the influence of TST volume on the performance of PVT systems mainly through modeling and simulation, and some experimental validations of dynamic models have been reported (Sredenšek et al., 2021), no comparative experimental study has yet directly assessed the impact of reducing TST volume on overall system performance. In this context, the present study provides an experimental comparison of a PVT system operating with two TST configurations, focusing on the influence of TST volume on the system's electrical and thermal performance under real operating conditions.

2. Methodology

2.1 General Description of the Experimental System

The experimental setup is located at the Laboratory of Energy Conversion Processes and Technology (LEPTEN) at the Federal University of Santa Catarina (UFSC), in Florianópolis, Brazil. The city has a humid subtropical climate, characterized by significant seasonal variations in temperature and solar irradiance. However, in the present study, the experiments were carried out during the summer period, when solar irradiance reaches its highest values.

The system consists of a PV module with a polypropylene HX with rectangular parallel channels attached to its rear surface. To mitigate the increase in PV cell temperature, water circulates through the channels, driven by a pump. As the fluid passes through the HX, it absorbs the excess thermal energy, lowering the temperature of the cells while simultaneously transferring useful heat to the TST.

The PVT system operation is illustrated in Figure 1, which shows a schematic representation of the system highlighting the simultaneous conversion of electricity and heat, and the integration of the module with the TST.

The system operated in an open-loop configuration without consumption, maintaining constant flow conditions during the tests. To ensure minimal external interference, the experiments were conducted without replenishment from the supply tank and with the discharge line fully closed, eliminating any water consumption during the experimental period.

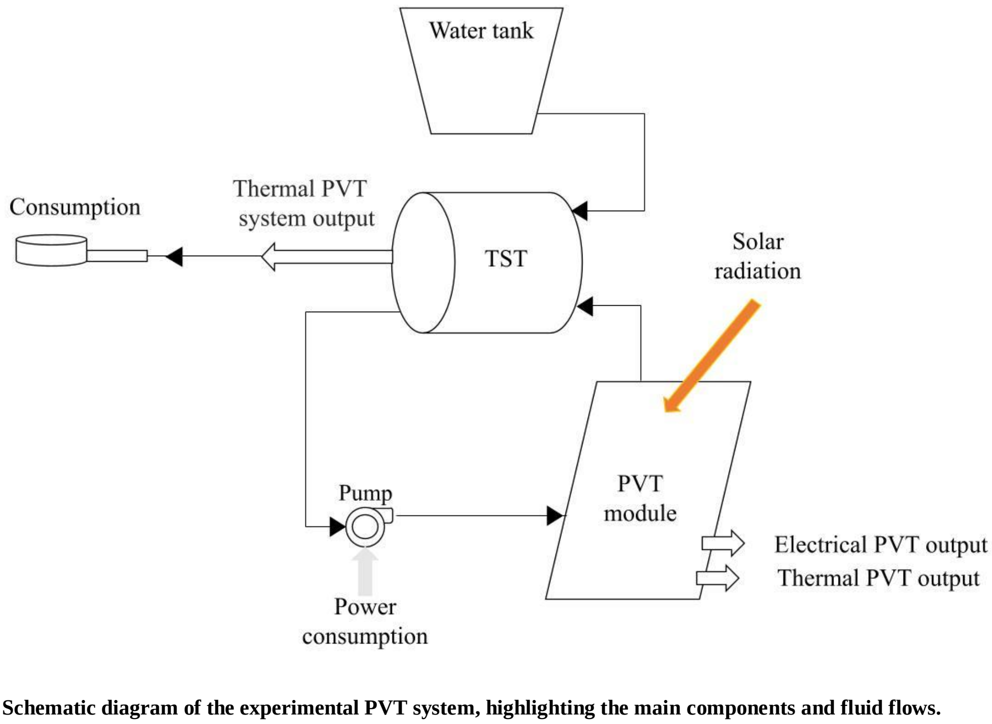

Figure 1: Schematic diagram of the experimental PVT system, highlighting the main components and fluid flows.

In addition, a thermal camera image compares the surface of a conventional PV module with that of a module equipped with the HX, confirming the ability of the device to cool the PV cells during operation, as can be seen in Figure 2.

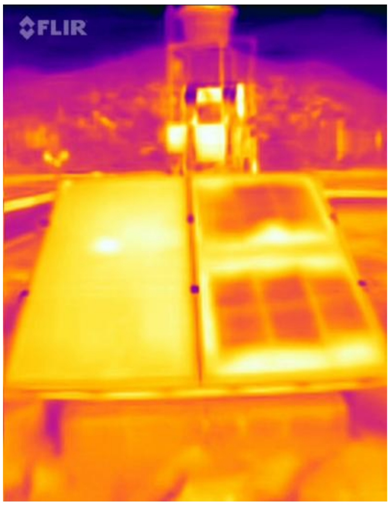

Figure 2: Thermal image comparing a conventional PV module (left) and the PVT module with heat exchanger (right), showing the cooling effect on the photovoltaic surface.

Beyond this general configuration, initially, the system employed a 300 L TST, with which several experimental tests were conducted and previous studies were published (Busson et al., 2023; Busson et al., 2024; Pereira da Cruz et al., 2024).

Subsequently, the infrastructure was reformulated, preserving as much as possible the original physical and construction characteristics. Although the polyethylene pipelines were renewed, the most significant modification consisted of replacing the 300 L TST with a 100 L one, enabling a comparison between the effects of two different TST volumes on water tank temperature and the PVT system performance. This difference between the test benches can be observed in Figures 3a and 3b, which highlight the preservation of the overall system configuration and the replacement of the TST.

a	b

Figure 3: Experimental PVT setup: (a) configuration with 300 L thermal storage tank; (b) configuration with 100 L thermal storage tank.

2.2 System Characteristics

The most relevant component for this study is the TST, since its volume was the main variable under investigation. Two configurations were tested: one with a 300 L TST and another with a 100 L TST. The dimensions, capacities, and specifications of both TSTs are summarized in Table 1.

Table 1: Specifications of the 300 L and 100 L TSTs.

Characteristic	300 L TST	100 L TST
Tank material	Stainless steel 316	Stainless steel 304
Dimensions (⌀ × h)	55 cm × 135 cm	40 cm × 90 cm
Thermal insulation	Polyurethane foam (50 mm)	Polyurethane foam (50 mm)
External coating	Aluminum	Aluminum
Hydraulic connections	Inlet: 1″ BSP / Outlet: 3/4″ BSP	Inlet: 1″ BSP / Outlet: 3/4″ BSP

The PV module used was a Canadian Solar CS3W polycrystalline panel, with a nominal power of 405 W under Standard Test Conditions, a nominal efficiency of 18.3%, and external dimensions of 2108 × 1048 × 40 mm, corresponding to an effective area of 2.21 m². These specifications were considered in the analysis of electrical performance and in the calculation of instantaneous electrical efficiency. The modules were installed with a fixed tilt angle of 27°, corresponding to the latitude of Florianópolis, ensuring proper alignment for solar radiation capture.

Water circulates through the HX channels, driven by a Lorenzetti BCL 6 circulation pump used for forced circulation. In the present experiment, the pump operated with its selector set to position 3, ensuring stable flow conditions through the HX and the TST.

Temperature measurements were performed using platinum resistance temperature detectors of type Pt100 (100 Ω at 0°C), Class A according to IEC 60751. The sensors have an intrinsic tolerance of ±(0.15 + 0.002|T|) °C, where *T* is the measured temperature in °C. Within the operating range of this study (approximately 15°C to 60°C), the uncertainty of the sensors ranged between ±0.18 °C and ±0.27°C.

Solar irradiance was monitored using an EKO MS-60 pyranometer, installed in the same tilted plane as the module (27°). Classified as First Class according to ISO 9060, the sensor has a measurement range of 0–2000 W m^{-2} and a spectral response between 285 and 3000 nm, fully adequate for outdoor solar applications. Previous studies in Brazil have reported that even under extreme overirradiance events caused by cloud reflections, peaks rarely exceed 1590 W m^{-2}, which remains comfortably within the sensor's capacity (Almeida et al., 2014). The associated uncertainty, considering directional response, non-linearity, and annual stability, lies within ±2 to ±3%.

The water flow rate was kept constant during all tests by controlling the tank outlet valve and the pump setting. The average operating flow was 7.1 (litre min^{-1}), measured with an Endress+Hauser Picomag electromagnetic flow meter (model DMA), which has a manufacturer-specified accuracy of ±0.8 % o.r. ±0.1 % o.f.s**.**

2.3 Monitored Variables and Data Processing

The variables monitored during the experiments included solar irradiance, ambient temperature, inlet and outlet water temperatures at the HX, internal temperature of the TST, electrical power output of the PV module, and the water mass flow rate. Data were recorded every 10 seconds by the acquisition system, generating high-resolution time series capable of capturing the dynamic behavior of the system. To compare the 100 L and 300 L configurations, five consecutive days of tests were conducted for each case, and only days with similar irradiance profiles were selected, as summarized in Table 2.

Table 2: Solar irradiation level in a tilted surface on selected test days.

Tests with 100 L TST (year 2025)	Irradiation ($kW\ h\ m^{-2}$)	Tests with 300 L TST (year 2024)	Irradiation ($kW\ h\ m^{-2}$)
01/03	6.80	26/03	6.93
02/03	7.58	14/03	7.57
03/03	7.30	12/03	7.42
04/03	6.66	15/03	6.53
05/03	6.83	27/03	7.20

Before calculating performance indices, the raw data were subjected to preprocessing. Measurements with irradiance values below 100 W m^{-2} were discarded to avoid distortions at sunrise and sunset, while spurious peaks caused by sensor response or communication errors were filtered out. A moving-average smoothing filter was then applied to reduce short-term oscillations and highlight overall trends.

The instantaneous thermal efficiency of the system was calculated according to Eq. (1):

$$\eta_{th(t)} = \frac{\dot{m}\ c\ (T_{out} - T_{in})}{G(t)A} \qquad \text{(eq. 1)}$$

where is $\dot{m}$ the mass flow rate of water (kg s^{-1}), c is the specific heat of water (4186 J kg^{-1} K^{-1}), T_{out} and T_{in} are the outlet and inlet temperatures at the HX (K), $G(t)$ is the solar irradiance (W m^{-2}), and A is the effective area of the module (m^2).

The instantaneous electrical efficiency was obtained using Eq. (2):

$$\eta_{el(t)} = \frac{P_{el(t)}}{G(t)A} \qquad \text{(eq. 2)}$$

where $P_{el(t)}$ is the electrical power provided by the data acquisition system, expressed in watts (W).

For the analysis of the water temperature inside the TST, data from the five testing days were plotted individually for each configuration, resulting in ten curves in total (five for the 100 L and five for the 300 L TSTs). This representation highlights the daily variability and the different thermal dynamics associated with each storage volume. Additionally, the TST water temperatures were averaged across the five days, producing representative hourly curves that provide a clearer comparison of the heating behavior of the 100 L and 300 L TSTs.

In terms of electrical performance, irradiance and electrical power data were grouped by day for each configuration. At each time step, the mean value across the five days was calculated, generating representative irradiance and power curves. The instantaneous electrical efficiency was then obtained from these averaged variables using Eq. (2), and the resulting curves were smoothed with a moving average filter to reduce random fluctuations and emphasize overall trends.

For the thermal performance, the same methodology was applied using the mass flow rate and the temperature difference between the inlet and outlet water at the HX. Since higher variability was observed outside the central hours of the day, the analysis was restricted to the period between 09:00 and 16:00 h, when measurements were more stable and representative of typical operating conditions. The instantaneous thermal efficiency was then determined using Eq. (1), after averaging across the five testing days for each configuration and applying the same moving average smoothing.

3 Results

The internal temperature of the TSTs over five consecutive test days exhibited a consistent pattern across both configurations. The 100 L TST heated more rapidly, reaching higher temperatures and surpassing 40°C on all analyzed days, whereas the 300 L TST warmed more gradually, never exceeding 40°C, and showed smaller thermal fluctuations. These trends are illustrated in Figure 4, which presents the TST water temperature profiles for each test day.

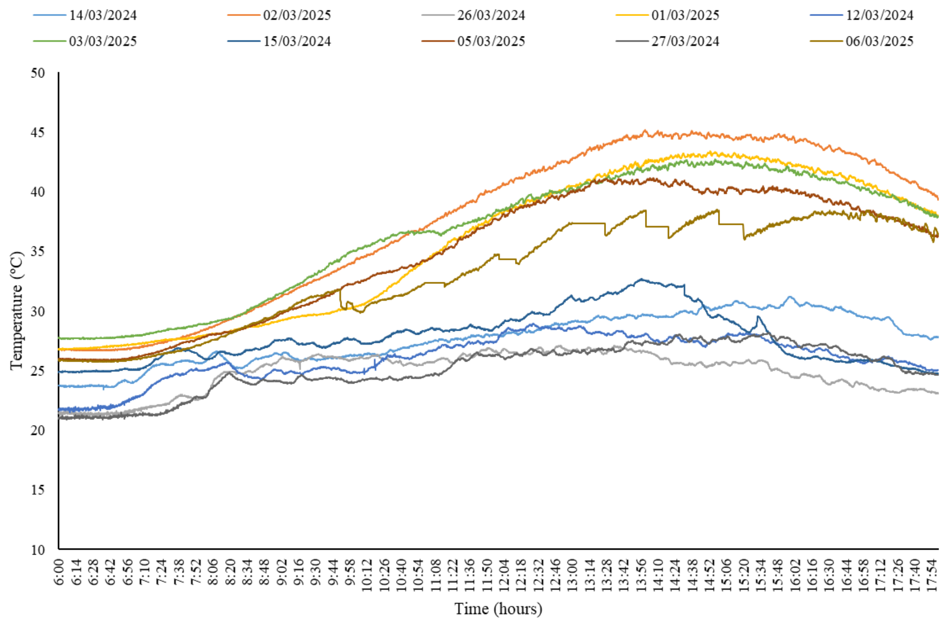

Figure 4: Tank temperature for 300 L and 100 L setups over the days analysed.

For a consolidated analysis, average temperature curves were obtained from the five test days for each configuration. The observed behavior confirmed the daily trend: the 100 L TST displayed a higher heating rate and larger thermal amplitudes, while the 300 L TST exhibited slower heating and greater stability throughout the day. Figure 5 presents these averaged curves, highlighting that the TST volume directly affects the system's thermal inertia, acting as a determining factor in the water-heating dynamics. Since the daily profiles showed behavior consistent with the averaged curves throughout the test period, the performance analyses presented in the following sections are based on averaged curves for each configuration.

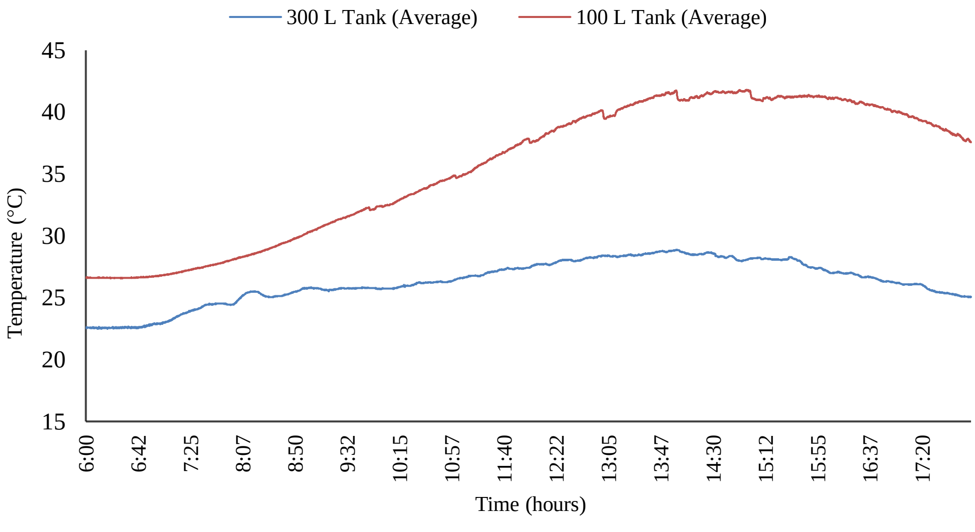

Figure 5: Average temperature curves of the 300 L and 100 L storage tanks, based on five test days.

When comparing the two configurations, it was observed that, for most of the day, the electrical efficiencies were similar, with only minor differences in the morning and early afternoon. However, from 16:00 h onward, the system with the 300 L TST achieved superior performance compared to the 100 L TST. This behavior is associated with the higher thermal inertia of the 300 L TST, already evidenced in the temperature analysis, which maintained lower water temperatures for a longer period and consequently prolonged the cooling effect on the PV cells under lower irradiance conditions. These results are illustrated in Figure 6.

The electrical efficiency values were calculated using Eq. (2), based on the measured electrical output and incident irradiance. On average, the electrical efficiency of the system with the 300 L TST was 15.85%, while the 100 L TST reached 15.18%, corresponding to an approximate 4.23% reduction in electrical performance with the smaller reservoir.

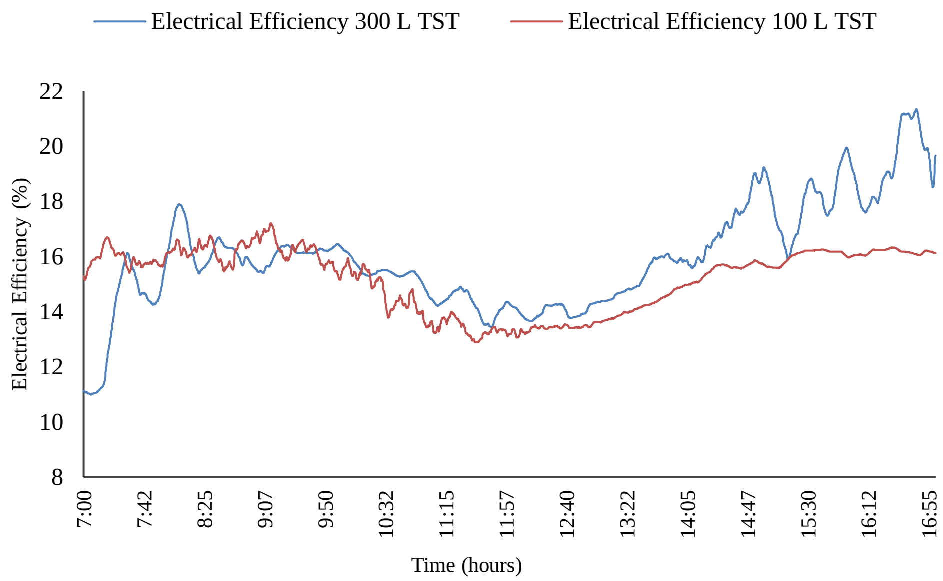

Figure 6: Average electrical efficiency profiles of the system with 300 L and 100 L storage tanks

The comparison between the two configurations also shows that the 100 L TST achieved higher thermal efficiency in the early morning and late afternoon, due to the larger temperature gradient between the colder water and the heated module. However, between approximately 10:00 and 14:00 h, when solar irradiance was more intense, the system with the 300 L TST performed better, sustaining higher and more stable values throughout this interval. These results are illustrated in Figure 7.

The thermal efficiencies were calculated using Eq. (1) and, on average, were 25.16% for the 100 L TST and 24.76% for the 300 L TST, representing a difference of about 1.62% between the two reservoirs**.** Nevertheless, the proximity between the average values indicates that the influence of storage volume on thermal efficiency is limited, being more relevant in the dynamic behavior throughout the day.

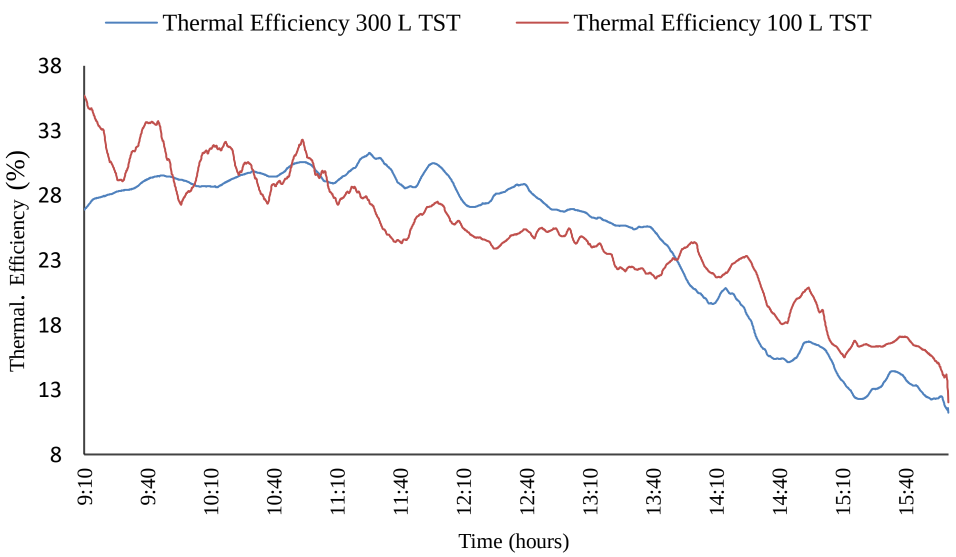

Figure 7: Average thermal efficiency profiles of the system with 300 L and 100 L storage tanks

The ambient temperatures recorded during the experimental campaigns of 2024 and 2025 were slightly higher in 2025, when the 100 L TST was tested. To verify whether this difference could significantly affect the results, the days of 15 March 2024 and 5 March 2025 were compared, as they presented similar irradiance and ambient temperature conditions.

The behavior observed for reservoir temperature, as well as for electrical and thermal efficiencies, followed the same patterns obtained from the averaged curves. This confirms that the increase in ambient temperature in 2025 did not exert a relevant impact on system performance, serving only as complementary information for contextualizing the experiments.

5. Conclusion

The experimental results showed that reducing the TST volume from 300 L to 100 L modified the thermal and electrical dynamics of the PVT system. The smaller TST exhibited faster heating and larger thermal amplitudes throughout the day, which slightly favored thermal efficiency. On the other hand, the higher water temperature reduced the cooling capacity of the PV cells, resulting in lower electrical efficiency. Thus, an inverse behavior between thermal and electrical performance was observed, highlighting the key role of the TST's thermal inertia.

These trends are consistent with the parametric study by Barbu et al. (2020), which predicted through modeling that larger TSTs favor thermal stability and electrical performance, while smaller TSTs reach higher temperatures in shorter intervals, partially benefiting the thermal fraction but penalizing the electrical side. In Barbu's work, variations of up to 4–5% in electrical efficiency were attributed to the reduction of TST volume, a value comparable to the 4.2% difference experimentally observed in the present study. Therefore, the results presented here provide experimental validation of theoretical trends previously reported in the literature, strengthening the understanding of the influence of TST volume on the overall performance of PVT systems.

However, defining an "ideal" volume is not straightforward, since electrical and thermal efficiencies do not reach their maximum simultaneously. The optimal TST volume depends on the prioritization criterion, maximizing electrical energy, useful heat, or an integrated metric (energetic, exergetic, or economic). For future work, it is recommended to investigate the combined effect of TST volume and domestic hot water consumption profiles to identify configurations that maximize overall energy utilization. In this sense, approaches that integrate experiments and modeling could establish practical guidelines for the optimal sizing of PVT systems in real-world applications.

6. Acknowledgments

The authors gratefully acknowledge the Laboratory of Energy Conversion Processes and Technology (LEPTEN) at the Federal University of Santa Catarina (UFSC) for providing the facilities and technical support required for this research.

The authors acknowledge the financial support of the Human Resources Program of the National Agency of Petroleum, Natural Gas and Biofuels (PRH-ANP).

7. References

Al-Shamani, A.N., Sopian, K., Mat, S., Hasan, H.A., Abed, A.M. & Ruslan, M.H., 2016. Experimental studies of rectangular tube absorber photovoltaic thermal collector with various types of nanofluids under the tropical climate conditions. *Energy Conversion and Management*, 124, 528–542.

Almeida, M.P., Zilles, R. & Lorenzo, E., 2014. Extreme overirradiance events in São Paulo, Brazil. *Solar Energy*, 110, 168–173.

Atawi, I.E., Abuelrub, A., Al-Shetwi, A.Q. & Albalawi, O.H., 2024. Design of a wind-PV system integrated with a hybrid energy storage system considering economic and reliability assessment. *Journal of Energy Storage*, 81, 110405.

Barbu, M., Darie, G. & Siroux, M., 2020. A parametric study of a hybrid photovoltaic thermal (PVT) system coupled with a domestic hot water (DHW) storage tank. *Energies*, 13(24), 6481.

Busson, B., de Oliveira de Brito, U.H., Pigozzo Filho, V.C., Leyton Mopan, A. & Passos, J., 2025. Energy and exergy losses in photovoltaic-thermal module with polymeric heat exchanger. *Proceedings of the 27th International Congress of Mechanical Engineering (COBEM 2023)*.

Busson, B. de O., Cruz, R.P. da, Brito, U.H. de O. de & Faleiros, R.W., 2024. Electrical and thermal performance of a photovoltaic-thermal (PVT) module under different sky conditions. *Proceedings of the Brazilian Solar Energy Congress (CBENS 2024)*. [in Portuguese].

Cirrincione, L., Malara, C., Marino, C., Nucara, A., Peri, G. & Pietrafesa, M., 2020. Effect of the thermal storage dimensions on the performances of solar photovoltaic-thermal systems. *Renewable Energy*, 162, 2004–2018.

Erixno, O. & Rahim, N.A., 2020. A techno-environmental assessment of hybrid photovoltaic-thermal based combined heat and power system on a residential home. *Renewable Energy*, 156, 1186–1202. Michael, J.J., S., I. & Goic, R., 2015. Flat plate solar photovoltaic–thermal (PV/T) systems: a reference guide. *Renewable and Sustainable Energy Reviews*, 51, 62–88.

Samykano, M., 2023. Hybrid photovoltaic thermal systems: present and future feasibilities for industrial and building applications. *Buildings*, 13(8), 1950.

Pereira da Cruz, R., de Oliveira Busson, B., William Faleiros, R. & César Passos, J.,(n.d). Energy performance of a residential photovoltaic-thermal (PVT) system under real operating conditions. *Proceedings of the 12th Brazilian Congress on Research and Development in Petroleum and Gas (PdPetro)*. [in Portuguese].

Sredenšek, K., Seme, S., Štumberger, B., Hadžiselimović, M., Chowdhury, A. & Praunseis, Z., 2021. Experimental validation of a dynamic photovoltaic/thermal collector model in combination with a thermal energy storage tank. *Energies*, 14(23), 8162.

Tiwari, A.K., Chatterjee, K., Agrawal, S. & Singh, G.K., 2023. A comprehensive review of photovoltaic-thermal (PVT) technology: performance evaluation and contemporary development. *Energy Reports*, 10, 2655–2679.